IEICE Electronics Express, Vol.16, No.16, 1–6

LETTER

Capacitive probe-compensation-fed wideband patch antenna with U-shaped parasitic elements for 5G/WLAN/WiMAX applications

Huaxiao Lu[1a)], Fang Liu[1], Weimin Wang[1], Zhaodong Gao[1], Xia Bai[1], and Yuan'an Liu[1]

Abstract A novel single layer, single capacitive probe-compensation fed wideband patch antenna is presented and investigated. The antenna consists of a rectangular patch and two identical U-shaped parasitic patches. The two U-shaped patches are incorporated around the radiating edges and non-radiating edges of the rectangular patch. For maintaining a relatively small antenna size, the length and width of this rectangular patch are $1/2\lambda_g$ and $1/4\lambda_g$, respectively. A novel capacitive compensation technique, that is an annular gap which is concentric with the fed-probe, can introduce an annular gap capacitor to compensate the inductance caused by the fed-probe. By incorporating the U-shaped parasitic patches, an additional resonant frequency is introduced, which incorporates with the original resonant frequency produced by the rectangular patch, thus the wideband performance is achieved. The measured impedance bandwidth with $S_{11} \leq -10$ dB is 40% (1.99 GHz) from 4.03 to 6.02 GHz, which covers 4.8–4.99 GHz band of 5G operation in China, WLAN 5.2 GHz (5.15–5.35 GHz), WLAN 5.8 GHz (5.725–5.825 GHz), and WiMAX 5.5 GHz (5.25–5.85 GHz). The measured peak gain is 9.1 dBi. An equivalent circuit model is established to provide a clear physical insight into the operation of the proposed antenna.

Keywords: wideband, U-shaped parasitic patches, patch antenna, annular gap capacitance, probe-compensation

Classification: Microwave and millimeter-wave devices, circuits, and modules

1. Introduction

Modern high-speed wireless communication systems, such as 5G (the fifth-generation mobile communication), WLAN, and WiMAX wireless applications, require wideband antennas. Microstrip antennas are very attractive in wireless communication systems because they have the advantages of lightweight, low cost, low profile, compactness, and easy integration with active and passive circuits such as filters, amplifiers, oscillators, and mixers. However, the inherent drawback of patch antennas is the narrow bandwidth, which limits their applications in wireless communication systems. Many researchers have devoted to broaden the bandwidth, and some techniques have been proposed. Increasing the thickness of substrate with low permittivity. Cutting slots in a patch, such as E-shaped slot [1], V-slot [2], U-slot [3], a pair of wide silts [4] and so on. Incorporating coplanar [5, 6] or stacked [7, 8] parasitic elements, however, the driven patch and parasitic patches in [5] are all full-size conventional patches, which resultantly suffers from relatively larger antenna size. The usage of stacked structures can generally broaden the bandwidth of patch antennas effectively, however, a stacked structure suffers from difficulty in layer alignment, complex antenna structure, and high fabrication cost. Specific feeding types are widely used to broaden the bandwidth, such as L-shaped probe feed [9], T-shaped probe feed [10], meandering probe feed [11], hook-shaped probe feed [12] and so on. These feeding techniques can provide proximate coupling capacitance to compensate the inductance caused by the feed-probe, and wideband characteristics can be obtained. For instance, a L-shaped probe feed with an impedance bandwidth of 36% is reported in [9]. A meandering probe feed with an impedance bandwidth of 30% is reported in [11]. These antennas maintain single-layer and single-patch. Besides, aperture coupling feed [13] and other feeding types [14, 15] are also used to broaden the bandwidth of patch antennas. For instance, a patch antenna with an aperture-coupled feed and patches of different sizes is reported in [13], which has an impedance bandwidth of 31%. Unfortunately, all these feeding techniques above-mentioned introduce additional complex structures, difficulty in assembling, and high fabrication cost. Furthermore, these antennas do not base on simple theory to help their designs. Therefore, some progress should be made to design wideband antennas with simple structure and theoretical analysis.

In this work, a single layer and a single capacitive probe-compensation fed wideband patch antenna is presented and investigated. The antenna consists of a rectangular patch with a reduced size and two identical U-shaped parasitic patches. The U-shaped parasitic patches are incorporated around both the radiating edges and non-radiating edges of the rectangular patch. A novel capacitive compensation technique, that is an annular gap embedded in the rectangular patch, is used to introduce an annular gap capacitor to compensate the inductance caused by the fed-probe. An additional resonant frequency is introduced by the U-shaped parasitic patches, which incorporates with the original resonant frequency produced by the rectangular patch, thus the wideband performance is achieved. The annular gap is concentric with the fed-probe, and is located on the surface of the rectangular patch. Thus the usage of this annular gap have negligible added design complexity and fabrication cost, and making the antenna a simple single layer and a single feed. Although parasitic patches are incorporated, the size for the whole radiating element of

[1]School of Electronic Engineering, Beijing University of Posts and Telecommunications, Beijing 100876, China
a) huaxiaous@126.com

DOI: 10.1587/elex.16.20190362
Received June 2, 2019
Accepted June 21, 2019
Publicized July 24, 2019
Copyedited August 25, 2019

the proposed antenna is smaller than that of a conventional patch. The proposed antenna has the advantages of wideband performance, simple structure, small radiating element volume, and high gain. Furthermore, an equivalent circuit model is built to theoretically analyze the proposed antenna and better understand its working mechanism, and also to provide theoretical guidance to help the antenna's design.

2. Antenna design

2.1 Antenna configuration

The configuration of the proposed antenna is shown in Fig. 1. The antenna consists of a rectangular patch with an annular gap (denoted as the main patch) and two identical U-shaped parasitic elements. The annular gap which is embedded in the rectangular patch, is concentric with the fed-probe, and is located on the surface of the rectangular patch. Generally, the length and width of a conventional patch are close to $1/2\lambda_g$ (λ_g is the guided wavelength), respectively. But for the proposed antenna, in order to maintain a small size, the width W_R of the rectangular patch is reduced to $1/4\lambda_g$, and the length L_R of the rectangular patch is about $1/2\lambda_g$. The two U-shaped parasitic patches are placed in proximity of both the radiating edges and non-radiating edges of the rectangular patch. For easy fabrication with PCB technology, the rectangular patch and the two U-shaped patches are both printed on a low cost FR4 substrate with thin thickness of 0.8 mm, relative permittivity of 4.4, and loss tangent $\tan\sigma = 0.02$. Air, with thickness of 5 mm and relative permittivity $\varepsilon_r = 1$, is used as the substrate. A SMA connector whose inner and outer diameters are 1.2 mm and 4.2 mm, respectively, is used to connect the main patch. As can be observed from Fig. 1, the overall antenna is geometrically symmetric along the x-axis, which is useful to maintain low cross-polarization. The final dimensions of the proposed antenna are tabulated in Table I.

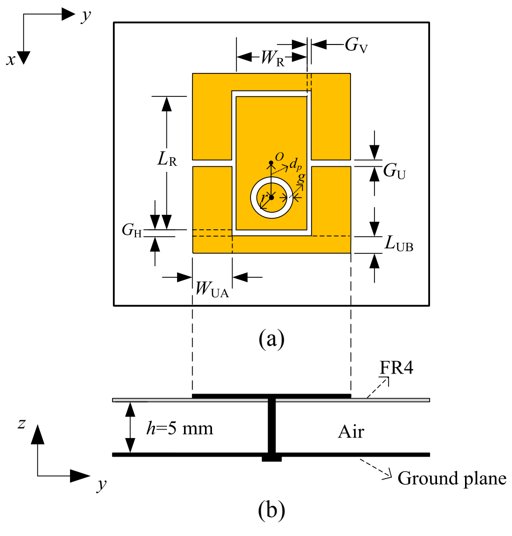

Fig. 1. The configuration of the proposed antenna: (a) top view; (b) side view.

Table I. The dimensions of the proposed antenna.

Parameter	L_R	W_R	d_p	r	g	G_V
Values (mm)	17.2	8.5	4.5	2	0.9	0.4
Parameter	G_U	G_H	W_{UA}	L_{UB}		
Values (mm)	0.8	0.9	5.7	3		

2.2 Working mechanism and theoretical analysis

As shown in Fig. 1, the rectangular patch loaded with the annular gap is the driven patch, and the two U-shaped patches are the parasitic patches. The annular gap etched in the rectangular patch can introduce an annular gap capacitor in series with the fed-probe, which is used to compensate the inductance caused by the fed-probe. The current distributions at the lower and higher resonant frequencies are shown in Fig. 2(a) and Fig. 2(b), respectively. As shown in Fig. 2(a), the current amplitudes on the two non-radiating edges of the main patch are strong, whereas on the U-shaped patches, are not strong. Therefore, the lower resonant frequency is determined by the main patch. As shown in Fig. 2(b), the current amplitudes around the four vertical gaps (G_V) and the two horizontal gaps (G_H) are strong. It suggests that the main patch capacitively couples energy to the U-shaped patches through these vertical gaps and horizontal gaps, thus the higher resonant frequency is produced, and can be controlled through adjusting the arm's length or the base of the U-shaped patches. It should be pointed out that wider variation of G_V or G_H is not suggested, otherwise, making the gain at the higher resonant frequency lower. After properly selecting the dimensions of the proposed antenna, the lower and higher resonant frequencies are merged together to achieve the wideband characteristic.

An equivalent circuit model will gradually be established to theoretically analyze the proposed antenna and also to better understand its working mechanism. The equivalent circuit model of the rectangular patch with the annular gap (the main patch), is shown in Fig. 3.

The parallel combination of $R_1L_1C_1$ elements presents the rectangular patch [16], and the inductor X_L presents the inductance caused by the fed-probe. X_L can be calculated by the formula (1) [17, 18].

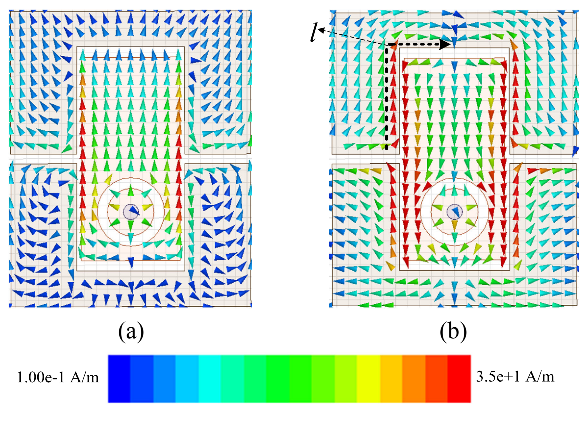

Fig. 2. The current distributions at: (a) 4.34 GHz; (b) 5.89 GHz.

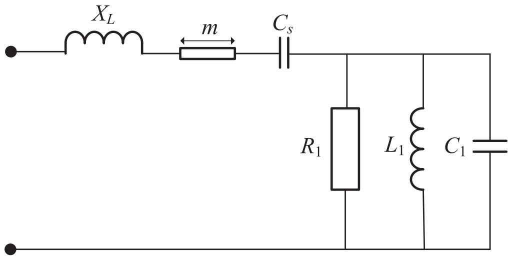

Fig. 3. Circuit model of the main patch using annular gap to compensate the inductance of the probe.

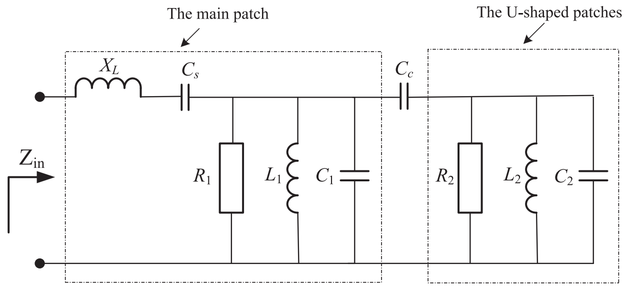

Fig. 4. Complete circuit model of the proposed antenna in Fig. 1

$$X_L = \frac{377 f_r h}{c_0} \ln \frac{c_0}{\pi f_r d_0 \sqrt{\varepsilon_r}} \tag{1}$$

In (1), d_0 is the diameter of the fed-probe, f_r is the operating frequency, h is the thickness of the substrate, and c_0 is the velocity of light in free space.

The annular gap which is concentric with the fed-probe, is described by its gap width g and inner radius r, can introduce an annular gap capacitor (denoted as C_s in Fig. 3) and a parallel plate radial microstrip line. The effect of this parallel plate radial microstrip line can be modeled by an additional transmission line of length m in the circuit model shown in Fig. 3. Furthermore, the effect of this transmission line can be neglected when the inner radius r is smaller in comparison to the thickness of the substrate [19]. The annular gap capacitor C_s can compensate the inductance caused by the fed-probe, thus C_s plays an important role in the antenna's impedance matching. C_s can be calculated by the approximated formulas (2)–(4) [20].

$$C_s = 2\pi r \cdot C(g, r, h, \varepsilon_r) \tag{2}$$

$$C(g, r, h, \varepsilon_r) \approx \frac{2\varepsilon_0 \varepsilon_{reff}}{\pi} \ln\left(\frac{8r}{g}\right) \tag{3}$$

$$\varepsilon_{reff} \approx 1 + \frac{\varepsilon_r - 1}{2} \frac{\ln\left(\frac{16h}{\pi g}\right)}{\ln\left(\frac{8r}{g}\right)} \tag{4}$$

It can be observed from (2)–(4) that C_s is determined by the inner radius r and the gap width g when the substrate has been selected. Furthermore, from (2)–(4), C_s increases when the combination of $r \ln(r)$ increases, which can be approximated locally by a linear line, and C_s decreases when the gap width g increases as expected. However, the dependence of C_s on g is only on its logarithm. Thus, the inner radius r plays a crucial role in controlling C_s, while the gap width g has moderate changes on C_s. These theoretical analysis on the capacitor C_s can provide guidance to design the antenna, and one can adjust the inner radius r, the gap width g, and the feed position to achieve an appropriate C_s to compensate the inductance caused by the fed-probe.

When incorporating the two U-shaped patches around both the radiating and non-radiating edges of the main patch, there is electromagnetic coupling between the main patch and the two U-shaped parasitic patches. This electromagnetic coupling is realized through the four vertical gaps (G_V) and the two horizontal gaps (G_H). Thus there is coupling capacitance (denoted as C_c in Fig. 4) between the main patch and the two U-shaped parasitic patches, which includes two parts. One is the coupling capacitance due to the four vertical gaps, which is mainly governed by the width (G_V) and the length ($(L_R - G_U)/2$) of the four vertical gaps as shown in Fig. 1, and increases with the decrease of the width (G_V) (or with the increase of the length ($(L_R - G_U)/2$). The other is the coupling capacitance due to the two horizontal gaps, which is mainly governed by the width (G_H) and the length (W_R) of the two horizontal gaps as shown in Fig. 1, and increases with the decrease of the width (G_H) (or

$$C_2 = \varepsilon_e \varepsilon_0 2 \cdot \left[2 \cdot \left(\frac{1}{2} L_R - \frac{1}{2} G_U + G_H + L_{UB}\right) \cdot W_{UA} + (W_R + 2 \cdot G_V) \cdot L_{UB}\right] \Big/ 2h \tag{5}$$

$$\varepsilon_e = \frac{\varepsilon_r + 1}{2} + \frac{\varepsilon_r - 1}{2} \left(1 + \frac{12h}{W_R}\right)^{-\frac{1}{2}} \tag{6}$$

with the increase of the length W_R). The two U-shaped patches can be modeled as the parallel combination of $R_2 L_2 C_2$ as shown in Fig. 4, wherein R_2, L_2, and C_2 present the equivalent resistor, the equivalent inductance, and the parallel plate capacitance of the U-shaped patches, respectively. Indeed, C_2 can be calculated by the formulas (5)–(6). L_2 corresponds to the surface current path length l of the U-shaped patches as shown in Fig. 2(b) (l is mainly determined by its part where the current distribution on the U-shaped patch is strong, that is the arm's length of the U-shape patch), and is increased with the increment of l, and vice versa. R_2 is increased as the thickness h of the substrate is increased (or as the quality factor Q of the proposed antenna is increased). So far, the complete equivalent circuit model of the proposed antenna has been established in Fig. 4.

2.3 Parametric studies

Parametric studies on parameters L_R and W_{UA} are carried out to study how they affect the antenna's performance.

Fig. 5 shows the simulated reflection coefficients (S_{11}) of the proposed antenna with the variation of L_R. Observe that with the increase of L_R, the lower and higher resonant frequencies both shift to lower frequency considerably. This is because that the lower resonant frequency is determined by the main patch, thus with the increase of L_R, the downward frequency shifts for the lower resonant frequency is observed. Meanwhile, with the increase of L_R, accordingly, the arm's length of the U-shaped patches is lengthened. Thus the surface current path length l of the U-shaped patches is lengthened, resultantly, the downward frequency shifts for the higher frequency is also observed.

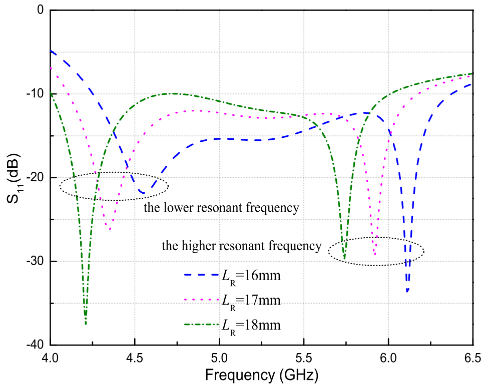

Fig. 5. The simulated reflection coefficients (S_{11}) with the variation of L_R.

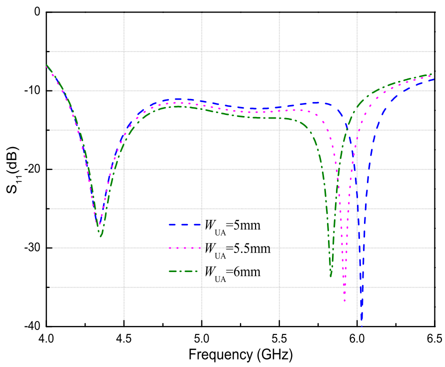

Fig. 6. The simulated reflection coefficients (S_{11}) with the variation of W_{UA}.

Fig. 6 shows the simulated reflection coefficients (S_{11}) of the proposed antenna with the variation of W_{UA}. It can be observed that with the increase of W_{UA}, the lower resonant frequency is almost kept unchanged, whereas the higher resonant frequency shifts to lower frequency moderately. This is because that with the increase of W_{UA}, the resonant length L_R of the main patch is kept unchanged, thus the lower resonant frequency is almost kept unchanged. However, with the increase of W_{UA}, the surface current path length l is lengthened, thus the downward frequency shifts for the higher resonant frequency is observed.

3. Results and discussions

The prototype of the proposed antenna is shown in Fig. 7. The measured and simulated reflection coefficients (S_{11}) of the antenna are shown in Fig. 8, observe that they are in good agreement. The measured impedance bandwidth with $S_{11} \leq -10$ dB is 40% (1.99 GHz) from 4.03 to 6.02 GHz, which covers 4.8–4.99 GHz band of 5G operation in China, WLAN 5.2 GHz (5.15–5.35 GHz), WLAN 5.8 GHz (5.725–5.825 GHz), and WiMAX 5.5 GHz (5.25–5.85 GHz) bands. The simulated impedance bandwidth with $S_{11} \leq -10$ dB is 40% (2.05 GHz) from 4.11 to 6.16 GHz. The two measured resonant frequencies are 4.45 GHz and 5.88 GHz, respectively, and those simulated ones are 4.34 GHz and 5.89 GHz, respectively. The discrepancy between the measured and simulated reflection coefficients (S_{11}) of the antenna is due to the fabrication tolerance and assemble error. The influence of the annular gap on the Z-parameter is simulated and shown in Fig. 9, by etching the annular gap, more gentle impedance curves are achieved.

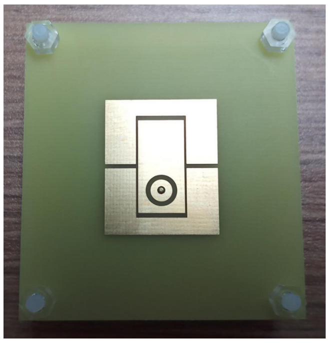

Fig. 7. Photograph of the proposed antenna.

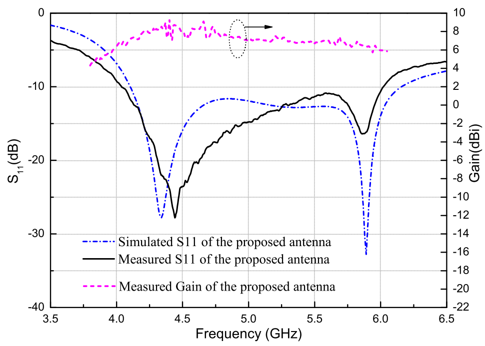

Fig. 8. The measured and simulated reflection coefficients (S_{11}), the measured gain of the proposed antenna.

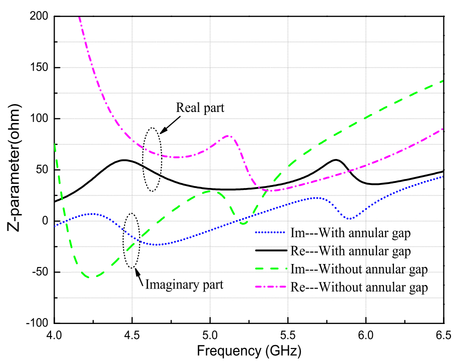

Fig. 9. The simulated Z-parameter of the proposed antenna with and without the annular gap

The measured and simulated radiation patterns in the xoz-planes and yoz-planes at 4.45 GHz and 5.88 GHz, are shown in Fig. 10 and Fig. 11, respectively. It can be observed that in all xoz-planes and yoz-planes, the measured and simulated co-polarization patterns are in good agreement. The measured and simulated radiation patterns for both the co-polarization and cross-polarization in all the

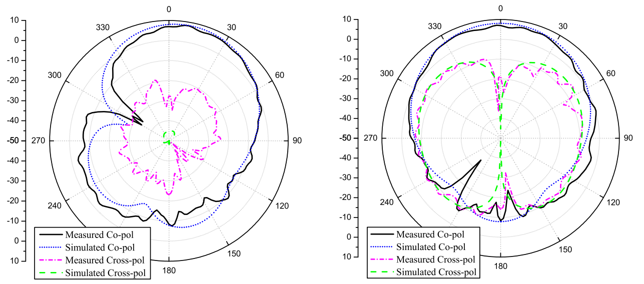

(a) (b)

Fig. 10. The measured and simulated radiation patterns at 4.45 GHz: (a) *xoz*-plane; (b) *yoz*-plane.

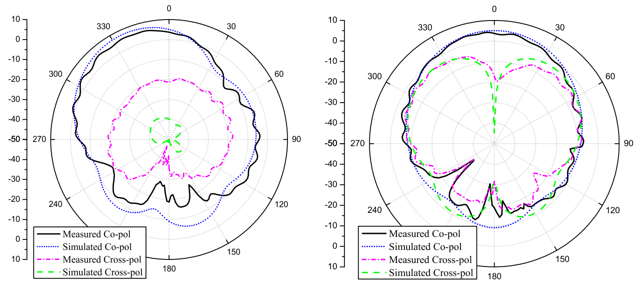

(a) (b)

Fig. 11. The measured and simulated radiation patterns at 5.88 GHz: (a) *xoz*-plane; (b) *yoz*-plane.

Table II. Comparisons with previous works

Ref	**Feed mechanism**	**Antenna configuration**	**Bandwidth (%) & Frequency range (or center frequency)**	**Radiating elements volume (mm^3) (λ_g is the wavelength in substrate at center frequency)**	**Gain (dBi)**
[8]	Meandering probe	Stacked	40%(1.575–2.36 GHz)	$61 \times 61 \times 26$ ($0.4\lambda_g \times 0.4\lambda_g \times 0.17\lambda_g$)	9
[9]	L-shaped probe	Single layer	36%(4.5 GHz)	$30 \times 25 \times 6.6$ ($0.45\lambda_g \times 0.375\lambda_g \times 0.1\lambda_g$)	7
[11]	M-shaped probe	Single layer	30%(1.56–2.12 GHz)	$70 \times 60 \times 17.5$ ($0.43\lambda_g \times 0.37\lambda_g \times 0.1\lambda_g$)	9
[13]	Aperture coupled	Single layer	31%(6–8.2 GHz)	$37 \times 19 \times 3.5$ ($1.48\lambda_g \times 0.76\lambda_g \times 0.14\lambda_g$)	8
[21]	L-shaped probe	Stacked	33%(1.72–2.4 GHz)	$52 \times 86 \times 30.2$ ($0.36\lambda_g \times 0.59\lambda_g \times 0.21\lambda_g$)	9.5
This work	Single probe	Single layer	40%(4.03–6.02 GHz)	$25 \times 20.7 \times 5.8$ ($0.42\lambda_g \times 0.35\lambda_g \times 0.1\lambda_g$)	9.1

yoz-planes, are symmetric. The measured peak gain across the bandwidth is shown in Fig. 8. It can be observed that the measured gains at the two resonant frequencies 4.45 GHz and 5.88 GHz are 8.7 dBi and 6.4 dBi, respectively.

The comparison between the proposed antenna and the previous antennas is shown in Table II. Observe that the proposed antenna has wide bandwidth, simple structure, small radiating element volume, and high gain.

4. Conclusion

A novel single layer and single capacitive probe-fed wideband patch antenna with two U-shaped parasitic patches is presented and investigated. An annular gap is etched in the rectangular patch, which can introduce an annular gap capacitor to compensate the inductance caused by the fed-probe. The usage of this annular gap has negligible added design complexity and fabrication cost, and resulting in a simple single layer and a single feed. The measured impedance bandwidth is 40% (1.99 GHz) from 4.03 to 6.02 GHz, which covers 4.8–4.99 GHz band of 5G operation in China, WLAN 5.2 GHz (5.15–5.35 GHz), WLAN 5.8 GHz (5.725–5.825 GHz), and WiMAX 5.5 GHz (5.25–5.85 GHz) bands. An equivalent circuit model is established to theoretically analyze the antenna. The proposed antenna has the advantages of wideband performance, simple structure, small size, and high gain, which can be a good candidate for 5G, WLAN, and WiMAX applications.

Acknowledgments

This work was supported in part by the National Natural Science Foundation of China (No. 61821001 and No. 61701041), and in part by the Beijing Key Laboratory of Work Safety Intelligent Monitoring (Beijing University of Posts and Telecommunications).

References

[1] F. Yang, *et al.*: "Wide-band E-shaped patch antennas for wireless communications," IEEE Trans. Antennas Propag. **49** (2001) 1094 (DOI: 10.1109/8.933489).

[2] A. A. Deshmukh and G. Kumar: "Broadband compact V-slot loaded RMSAs," Electron. Lett. **42** (2006) 951 (DOI: 10.1049/el:20061141).

[3] K. F. Lee, *et al.*: "Experimental and simulation studies of the coaxially fed U-slot rectangular patch antenna," IEE Proc., Microw. Antennas Propag. **144** (1997) 354 (DOI: 10.1049/ip-map:19971334).

[4] K.-L. Wong and W.-H. Hsu: "A broad-band rectangular patch antenna with a pair of wide slits," IEEE Trans. Antennas Propag. **49** (2001) 1345 (DOI: 10.1109/8.951507).

[5] G. Kumar and K. Gupta: "Broad-band microstrip antennas using additional resonators gap-coupled to the radiating edges," IEEE Trans. Antennas Propag. **32** (1984) 1375 (DOI: 10.1109/TAP.1984.1143264).

[6] J. D. Zhang, *et al.*: "A compact microstrip-fed patch antenna with enhanced bandwidth and harmonic suppression," IEEE Trans. Antennas Propag. **64** (2016) 5030 (DOI: 10.1109/TAP.2016.2618539).
[7] B.-L. Ooi, *et al.*: "Novel design of broad-band stacked patch antenna," IEEE Trans. Antennas Propag. **50** (2002) 1391 (DOI: 10.1109/TAP.2002.802087).
[8] H. W. Lai and K. M. Luk: "Wideband stacked patch antenna fed by meandering probe," Electron. Lett. **41** (2005) 297 (DOI: 10.1049/el:20057671).
[9] C. L. Mak, *et al.*: "Experimental study of a microstrip patch antenna with an L-shaped probe," IEEE Trans. Antennas Propag. **48** (2000) 777 (DOI: 10.1109/8.855497).
[10] C. L. Mak, *et al.*: "Broadband patch antenna with a T-shaped probe," IEE Proc., Microw. Antennas Propag. **147** (2000) 73 (DOI: 10.1049/ip-map:20000264).
[11] H. W. Lai and L. Kwai-Man: "Design and study of wide-band patch antenna fed by meandering probe," IEEE Trans. Antennas Propag. **54** (2006) 564 (DOI: 10.1109/TAP.2005.863091).
[12] A. A. Kishk, *et al.*: "A wide-band small size microstrip antenna proximately coupled to a hook shape probe," IEEE Trans. Antennas Propag. **52** (2004) 59 (DOI: 10.1109/TAP.2003.820979).
[13] Y. Jia, *et al.*: "Slot-coupled broadband patch antenna," Electron. Lett. **51** (2015) 445 (DOI: 10.1049/el.2014.3905).
[14] W. An, *et al.*: "Low-profile and wideband microstrip antenna with stable gain for 5G wireless applications," IEEE Antennas Wireless Propag. Lett. **17** (2018) 621 (DOI: 10.1109/LAWP.2018.2806369).
[15] W. An, *et al.*: "Low-profile and wideband dipole antenna with unidirectional radiation pattern for 5G," IEICE Electron. Express **15** (2018) 20180121 (DOI: 10.1587/elex.15.20180121).
[16] P. B. Garg, *et al.*: *Microstrip Antenna Design Handbook* (Artech House, Norwood, MA, 2001) 1st ed.
[17] V. G. Kasabegoudar and K. J. Vinoy: "Coplanar capacitively coupled probe fed microstrip antennas for wideband applications," IEEE Trans. Antennas Propag. **58** (2010) 3131 (DOI: 10.1109/TAP.2010.2055781).
[18] H. Malekpoor and S. Jam: "Analysis on bandwidth enhancement of compact probe-fed patch antenna with equivalent transmission line model," IET Microw. Antennas Propag. **9** (2015) 1136 (DOI: 10.1049/iet-map.2014.0384).
[19] M. Manteghi: "Analytical calculation of impedance matching for probe-fed microstrip patch antennas," IEEE Trans. Antennas Propag. **57** (2009) 3972 (DOI: 10.1109/TAP.2009.2033481).
[20] J. M. Kovitz and Y. Rahmat-Samii: "Using thick substrates and capacitive probe compensation to enhance the bandwidth of traditional CP patch antennas," IEEE Trans. Antennas Propag. **62** (2014) 4970 (DOI: 10.1109/TAP.2014.2343239).
[21] M. T. Islam, *et al.*: "Wideband stacked microstrip patch antenna for wireless communication," 2008 IEEE International Symposium on Parallel and Distributed Processing with Applications (2008) 547 (DOI: 10.1109/ISPA.2008.76).